Acta Crystallographica Section D
Biological Crystallography
ISSN 0907-4449

Structure of the CoA transferase from pig heart to 1.7 Å resolution

Abbie M. Coros,[a]‡ Lora Swenson,[b]§ William T. Wolodko[b] and Marie E. Fraser[a]*

[a]Department of Biological Sciences, University of Calgary, Calgary, AB T2N 1N4, Canada, and [b]Department of Biochemistry, University of Alberta, Edmonton, AB T6G 2H7, Canada

‡ Current address: Wadsworth Center, New York State Department of Health, Albany, NY 12201-2002, USA
§ Current address: Vertex Pharmaceuticals Inc., 130 Waverly Street, Cambridge, MA 02139, USA

Correspondence e-mail: frasm@ucalgary.ca

© 2004 International Union of Crystallography
Printed in Denmark – all rights reserved

Received 18 April 2004
Accepted 22 July 2004

PDB References: SCOT, 1ooy, r1ooysf; ΔSCOT, space group $P2_12_12$, 1ooz, r1oozsf; ΔSCOT, space group $C2$, 1ope, r1opesf.

Succinyl-CoA:3-ketoacid CoA transferase (SCOT; EC 2.8.3.5) activates the acetoacetate in ketone bodies by transferring the CoA group from succinyl-CoA to acetoacetate to produce acetoacetyl-CoA and succinate. In the reaction, a glutamate residue at the active site of the enzyme forms a thioester bond with CoA and in this form the enzyme is subject to autolytic fragmentation. The crystal structure of pig heart SCOT has been solved and refined to 1.7 Å resolution in a new crystal form. The structure shows the active-site glutamate residue in a conformation poised for autolytic fragmentation, with its side chain accepting one hydrogen bond from Asn281 and another from its own amide N atom. However, the conformation of this glutamate side chain would have to change for the residues that are conserved in the CoA transferases (Gln99, Gly386 and Ala387) to participate in stabilizing the tetrahedral transition states of the catalytic mechanism. The structures of a deletion mutant in two different crystal forms were also solved.

1. Introduction

Succinyl-CoA:3-ketoacid CoA transferase (SCOT; EC 2.8.3.5) is an essential enzyme in ketone-body metabolism. Ketone bodies, which are produced in the liver, serve as a source of fuel for extrahepatic tissues, such as the heart and the brain, during fasting or starvation. SCOT functions to activate the acetoacetate in ketone bodies by transferring the CoA group from succinyl-CoA to acetoacetate to produce acetoacetyl-CoA and succinate (Stern *et al.*, 1956). Acetoacetyl-CoA is further catabolized to acetyl-CoA, which enters the citric acid cycle or is used for fatty-acid metabolism. Mutations in SCOT have been detected in individuals who suffer from severe ketoacidosis in periods of fasting and disease (Kassovska-Bratinova *et al.*, 1996; Pretorius *et al.*, 1996; Niezen-Koning *et al.*, 1997; Snyderman *et al.*, 1998).

The transfer of CoA from one substrate to another occurs *via* a ping-pong mechanism (Hersh & Jencks, 1967) involving the formation of a covalent thioester bond between coenzyme A and a glutamate residue at the active site of the enzyme (Solomon & Jencks, 1969). The active-site glutamate residue of pig heart SCOT has been identified as Glu305 (Williams, 1990; Rochet & Bridger, 1994). When SCOT was incubated with acetoacetyl-CoA and succinate-^{18}O, the labelled O atom was transferred to the enzyme (Benson & Boyer, 1969). This suggested that the reaction proceeds through either a four-centred intermediate or a mixed anhydride between the carboxylate of the substrate and the active-site glutamate residue, with the free thiol of CoA then replacing the carboxylate to form the thioester (Benson & Boyer, 1969). The existence of the mixed anhydride is supported by more

recent oxygen-exchange studies with a bacterial CoA transferase, glutaconate CoA transferase from *Acidaminococcus fermentans* (GCT; Selmer & Buckel, 1999). GCT plays a role in the glutamate-fermentation pathway of *A. fermentans*, where it catalyzes the exchange of (*R*)-2-hydroxyglutarate to the CoA moeity of acetyl-CoA (Buckel *et al.*, 1981). In oxygen-exchange experiments, the distribution of labelled O atoms was measured by mass spectrometry after reacting acetate-^{18}O and glutaryl-CoA with the enzyme (Selmer & Buckel, 1999).

The structures of GCT (Jacob *et al.*, 1997), of pig heart SCOT (Bateman *et al.*, 2002) and of the α-subunit of *Escherichia coli* acetate CoA transferase (ACT; Korolev *et al.*, 2002) have been determined by X-ray crystallography. GCT and SCOT have the same fold, although the single 481-amino-acid polypeptide of SCOT corresponds to the two different subunits of GCT, as predicted by Jacob *et al.* (1997). The amino-terminal residues of SCOT superpose with residues of the α-subunit of GCT and the carboxy-terminal residues of SCOT superpose with residues of the β-subunit of GCT. The α-subunit of ACT (α-ACT) corresponds to the α-subunit of GCT (Korolev *et al.*, 2002). GCT is a heterooctamer, with four α-subunits and four β-subunits. Pig heart SCOT can exist as both a dimer and a tetramer (Rochet *et al.*, 2000), but the interpretation was that the initial crystal structure solved shows the dimer (Bateman *et al.*, 2002). The two monomers in the pig heart SCOT dimer interact in the same way that two $\alpha\beta$-heterodimers interact in the GCT structure (Bateman *et al.*, 2002).

The crystal structure of SCOT lends support to the catalytic roles hypothesized by Jacob and coworkers for several residues in the active site of the CoA transferases (Jacob *et al.*, 1997). As expected, Glu305 of SCOT superposes with residue 54β of GCT, which is known to be the active-site glutamate residue (Mack & Buckel, 1995). Other nearby residues that superpose and are identical in the two CoA transferases are Gln99 in SCOT and 103α in GCT, and Gly-Gly-Ala residues 385–387 in SCOT and 136–138β in GCT (Bateman *et al.*, 2002). Jacob and coworkers postulated that the amide N atoms of these residues would stabilize the developing negative charges on the carbonyl O atoms of the glutamyl thioester and of the carboxylate substrates in the tetrahedral transition states. Ser78α and Ser68β of GCT, two residues that are thought to interact with the glutaconate substrate (Jacob *et al.*, 1997), have no equivalent residues in SCOT (Bateman *et al.*, 2002). This comes as no surprise, since the carboxylate substrates of the two enzymes are quite different and therefore the substrate-binding pockets should be different.

Evidence for the existence of different conformations of SCOT has accumulated over the years. The enzyme was shown to be more 'open' when CoA was linked to the active-site glutamate residue, allowing labelling of a specific cysteine residue (White *et al.*, 1976). The amino- and carboxy-terminal portions of SCOT are normally connected by a hydrophilic linker, but this linker can be proteolytically cleaved with no effect on the activity of the enzyme (Lin & Bridger, 1992). Most recently, Shoolingin-Jordan and coworkers showed that although both of the active sites of SCOT can react with acetyl-CoA, only one of the glutamyl-CoA residues can subsequently react with succinate (Lloyd & Shoolingin-Jordan, 2001).

The crystal structure of pig heart SCOT described here shows the structure to high resolution, 1.7 Å, allowing us to delineate the structural features involved with the mechanism and autolytic fragmentation. We have also solved two structures of a mutant form of SCOT, ΔSCOT, in which six amino-acid residues were deleted from the linker (Rochet *et al.*, 2000).

2. Materials and methods

2.1. Expression and purification

The mature forms of SCOT and of the deletion mutant were produced and purified as described by Rochet *et al.* (2000). The mature form of SCOT is a protein of 481 amino-acid residues. For the deletion mutant, six residues in a region of SCOT that is easily cleaved by proteases were removed: residues 249–254 (Glu-Asp-Val-Lys-Thr-Arg). This mutant is identified as ΔSCOT in this paper.

2.2. Crystallization and X-ray data collection

Crystals of SCOT had first been grown using polyethylene glycol 2000 (P2K) as the precipitant, buffered by 4-(2-hydroxyethyl)-1-piperazine-ethanesulfonic acid (HEPES) at pH 7.5 (unpublished data). However, these crystals were difficult to work with because (i) they belonged to the monoclinic space group $P2_1$ with a 264 Å *b* axis and two SCOT dimers in the asymmetric unit and (ii) they were non-isomorphous to one another, as detected by native Patterson maps and difference statistics (unpublished data). While searching for better crystals, it was discovered that SCOT would also crystallize from P2K solutions buffered with phosphate. Crystals were grown in hanging drops that were set up by mixing 2 µl protein solution at a concentration of 7 mg ml^{-1} with 2 µl precipitant solution and suspended over 1 ml precipitant solution. The precipitant solution contained 3 m*M* sodium succinate, 16–18%(*w*/*v*) P2K and 100 m*M* (Na,K)PO_4. The (Na,K)PO_4 buffer was formed by mixing appropriate volumes of 4 *M* NaH_2PO_4 and 4 *M* K_2HPO_4 to achieve pH 7.5–8.0 and diluting this buffer in the precipitant solution. These crystals of SCOT grew as rectangular prisms or rectangular plates. The first data set was collected on beamline X12C at the National Synchrotron Light Source using the Brandeis 10 × 10 cm^2 CCD detector with the wavelength set to 1.1 Å. The crystal was prepared for data collection by transfer through solutions of increasing concentrations of MPD in the mother liquor to a maximum concentration of 10% MPD followed by vitrification in a nitrogen stream at 100 K. This data set, as well as subsequent ones, was indexed and processed using the programs *DENZO* and *SCALEPACK* (Otwinowski & Minor, 1997). The crystal form was orthorhombic, belonging to space group $P2_12_12$, and from the unit-cell parameters, which are listed in Table 1, it was calcu-

lated that there should be two monomers in the asymmetric unit.

The deletion mutant was crystallized under similar conditions. The largest rectangular plate (0.5 × 0.3 × 0.05 mm) grew from 2 µl 8 mg ml^{-1} protein solution mixed with 2 µl precipitant solution and suspended over 1 ml precipitant solution containing 23%(*w*/*v*) P2K, 100 m*M* (Na,K)PO_4 (pH 7.6 for the 4 *M* solution) and 0.05%(*w*/*v*) sodium azide. This crystal was transferred to cryosolutions that contained increasing concentrations of glycerol to a final concentration of 15%(*v*/*v*) glycerol in 20%(*w*/*v*) P2K, 100 m*M* (Na,K)PO_4 (pH 7.6 for the 4 *M* solution). The crystal was vitrified in the nitrogen stream at 100 K and the data were collected on the BioCARS beamline at the Advanced Photon Source with a wavelength of 1.00 Å using an ADSC Quantum-4 CCD detector. We also used crystals of the deletion mutant, ΔSCOT, in a search for isomorphous heavy-atom derivatives at the BioCARS beamline and discovered a second crystal form. (These data were collected before the structure of the selenomethionine version of the protein was solved; Bateman *et al.*, 2002). This second crystal form for the deletion mutant was monoclinic, space group *C*2, and was expected to contain two monomers in the asymmetric unit. The data set identified as ΔSCOT *C*2 was collected from a crystal that had been soaked in 0.05 m*M* mercury acetate in 20%(*w*/*v*) P2K, 100 m*M* (Na,K)PO_4 pH 7.5 and 0.05%(*w*/*v*) sodium azide for 21 h, washed with mother liquor containing no mercury acetate and transferred to solutions containing increasing amounts of glycerol to a final concentration of 20%(*v*/*v*) glycerol in 20%(*w*/*v*) P2K, 100 m*M* (Na,K)PO_4 pH 7.5.

Table 1
Statistics for the three data sets and for the refined models of wild-type pig heart CoA transferase (SCOT $P2_12_12$), the deletion mutant crystallized in space group $P2_12_12$ (ΔSCOT $P2_12_12$) and the deletion mutant crystallized in space group *C*2 (ΔSCOT C2).

	SCOT $P2_12_12$	ΔSCOT $P2_12_12$	ΔSCOT *C*2
Resolution limit (Å)	1.7	2.1	2.5
Unit-cell parameters			
a (Å)	99.45	96.82	147.64
b (Å)	140.32	139.11	68.70
c (Å)	68.10	68.48	103.50
α (°)	90	90	90
β (°)	90	90	99.58
γ (°)	90	90	90
No. measurements	321623	223149	63959
No. unique reflections	100807	53576	30903
$\langle I\rangle/\langle\sigma(I)\rangle$†	20.6	40.1	18.0
$\langle I\rangle/\langle\sigma(I)\rangle$ in high resolution shell (resolution range)	2.5 (1.73–1.70 Å)	9.2 (2.14–2.10 Å)	11.1 (2.59–2.50 Å)
R_{merge}‡ (%)	5.9	3.6	4.0
R_{merge} in high resolution shell (%) (resolution range)	21.6 (1.73–1.70 Å)	11.9 (2.14–2.10 Å)	8.6 (2.59–2.50 Å)
No. data for refinement	96525	51992	30523
Completeness (%)	91.6	94.9	85.6
R factor§ (%) (No. data)	15.6 (86808)	16.1 (46773)	18.0 (27430)
R_{free}¶ (No. data)	19.4 (9717)	21.0 (5219)	23.5 (3093)
No. protein atoms	7098††	7057‡‡	6994§§
No. water molecules	975	782	202
No. ions	5¶¶	3†††	6‡‡‡
R.m.s. deviations from ideal geometry			
Bond lengths (Å)	0.019	0.019	0.019
Bond angles (°)	2.0	2.0	2.0
Ramachandran plot statistics for non-proline and non-glycine residues			
No. in most favored regions	733 (92.4%)	737 (93.6%)	710 (91.6%)
No. in additional allowed regions	54 (6.8%)	46 (5.8%)	59 (7.6%)
No. in generously allowed regions	4 (0.5%)	2 (0.3%)	4 (0.5%)
No. in disallowed regions	2 (0.3%)	2 (0.3%)	2 (0.3%)
R.m.s. deviations in *B* values (Å^2)			
Main-chain atoms	0.90	0.96	1.0
Side-chain atoms	1.7	1.8	1.7
Average *B* values for water molecules (Å^2) (range)	29 (8–64)	28 (4–57)	22 (2–64)

† $\langle I\rangle$ is the mean intensity for all reflections, $\langle\sigma(I)\rangle$ is the mean sigma for these reflections. ‡ $R_{merge} = (\sum\sum|I_i - \langle I\rangle|)/\sum\sum\langle I\rangle$, where I_i is the intensity of an individual measurement of a reflection and $\langle I\rangle$ is the mean value for all equivalent measurements of this reflection. § *R* factor = $\sum||F_o| - |F_c||/\sum|F_o|$. ¶ *R* factor based on data excluded from the refinement (~10%). †† The residues modelled are 1–242 and 261–481 of chain *A* and 1–248 and 262–481 of chain *B*. There are two conformations for 170 of these atoms. ‡‡ The residues modelled are 1–246, 260–375 and 381–481 of chain *A* and 1–246, 260–375 and 382–481 of chain *B*. There are two conformations for 19 of these atoms. §§ The residues modelled are 1–135, 141–246, 262–376, 381–405 and 410–481 of chain *A* and 1–246, 262–406 and 410–481 of chain *B*. ¶¶ Four potassium ions and one phosphate ion. ††† Three potassium ions. ‡‡‡ Four mercury ions, bound to histidine residues, and two potassium ions.

2.3. Structure determination, refinement and analysis

The data were analyzed using programs from the *CCP*4 package (Collaborative Computational Project, Number 4, 1994) and the program *GLRF* (Tong & Rossmann, 1990). The structures were solved by the molecular-replacement method using the program *AMoRe* (Navaza, 1994). The search model for SCOT in the orthorhombic crystal form was one monomer, chain *A*, from the structure of the selenomethionine protein, which is identified by code 1m3e in the Protein Data Bank (Berman *et al.*, 2000). The model of SCOT was refined in the orthorhombic crystal form using the *Crystallography and NMR System* (*CNS*; Brünger *et al.*, 1998) with intervening steps of fitting the model to the electron-density maps using the program *TOM* (*ALBERTA*/*CALTECH* v.3.0) (Jones, 1985). The dimer from the orthorhombic crystal form was used as the search model to solve the structure of the deletion mutant in both the orthorhombic and monoclinic crystal forms. These models were fitted and refined in a similar manner to the model of SCOT. The quality of each model was judged using the programs *PROCHECK* (Laskowski *et al.*, 1993) and *WHATCHECK* (Hooft *et al.*, 1996). *WHATCHECK* was also used to determine optimal unit-cell parameters.

2.4. Modelling of the β-subunit of acetyl-CoA transferase from *E. coli*

Since the structure of the β-subunit of acetyl-CoA transferase has not been determined, it was modelled based on the structure of SCOT. Since the sequence similarity is high at 65% (44% identical for the 214 residues), *Swiss Modeller* could be used to build the model with no user intervention (Peitsch, 1995, 1996; Guex & Peitsch, 1997).

3. Results and discussion

3.1. Overview

The unit-cell parameters and the statistics for the data sets are presented in Table 1, along with summaries of the refined models. The coordinates as well as the structure-factor data have been submitted to the Protein Data Bank. The PDB identifiers are 1ooy for SCOT, 1ooz for ΔSCOT in space group $P2_12_12$ and 1ope for ΔSCOT in space group $C2$. In each structure, the two monomers in the asymmetric unit, identified as chains *A* and *B*, form a dimer in the same way that the pairs of chains, *A* and *B* and *C* and *D*, form dimers in the original structure of pig heart CoA transferase (Bateman *et al.*, 2002). In this discussion, the residue number followed by the chain label identifies residues, but the chain label is omitted if the description applies to both chains. Since the structure of SCOT is refined to the highest resolution, it is the primary structure described here.

Two residues, Asn190 of each monomer, have (φ, ψ) values that fall in the disallowed region of the Ramachandran plot and the residues are clearly defined in the electron density. Asn190 is located in a turn near the β-hairpin that supports the catalytic glutamate residue. Hydrogen-bonding interactions with the main-chain and the side-chain atoms appear to compensate for the destabilizing effect of the (φ, ψ) values.

3.2. Glu305, the active-site glutamate residue

The high-resolution structure of SCOT presents evidence for a detailed explanation of the autolytic fragmentation that is known to occur in this enzyme (Fig. 1). The autolytic fragmentation was demonstrated by Howard and coworkers, who postulated that any enzyme that had an activated glutamyl residue could undergo cyclization and cleavage of the peptide bond, analogous to the cyclization and cleavage seen in the plasma proteins, α_2-macroglobulin and complement components 3 and 4 (Howard *et al.*, 1986). In SCOT, the activated glutamyl residue is the thioester formed by attachment of CoA to the active-site glutamate residue, Glu305. In the structure of SCOT, the carboxylate group of Glu305 accepts a hydrogen bond from the side chain of Asn281 (2.9 Å), pulling the side chain of Glu305 over its amide N atom (Fig. 2). A similar conformation is seen in a glutamate residue of the canonical loop in the serine proteinase inhibitor turkey ovomucoid third domain (OMTKY3; Read *et al.*, 1983). In OMTKY3, the glutamate residue accepts a hydrogen bond from a threonine residue and this is thought to contribute to the rigidity of the loop that makes OMTKY3 a good inhibitor rather than a substrate. In SCOT, the carboxylate O atom (OE1) also accepts hydrogen bonds from at least one water molecule (2.8 Å) and from its own amide N atom (2.7 Å). Hence, the side chain of Glu305 is in a good conformation for attack by the amide N atom on the C atom of the thioester group to form a five-membered ring and its own side-chain O atom is in position to accept the hydrogen from the amide N atom. In the thioester, the S atom of CoA would replace the O atom OE2 of Glu305. The mechanism as proposed by Howard and coworkers proceeds through an oxyproline intermediate (Fig. 1) (Howard *et al.*, 1986). The main-chain atoms of Glu305 are in a conformation that could be adopted by the oxyproline intermediate, since the φ and ψ values are −70 and −14°, respectively, which are angles that are acceptable for a proline residue. At this stage, the CoA molecule could be released, leaving the 5-oxyproline residue. This unstable 5-oxyproline residue could be attacked by a water molecule at one of the two carbonyl C atoms, either reforming the native enzyme with free Glu305 at the active site or fragmenting the polypeptide

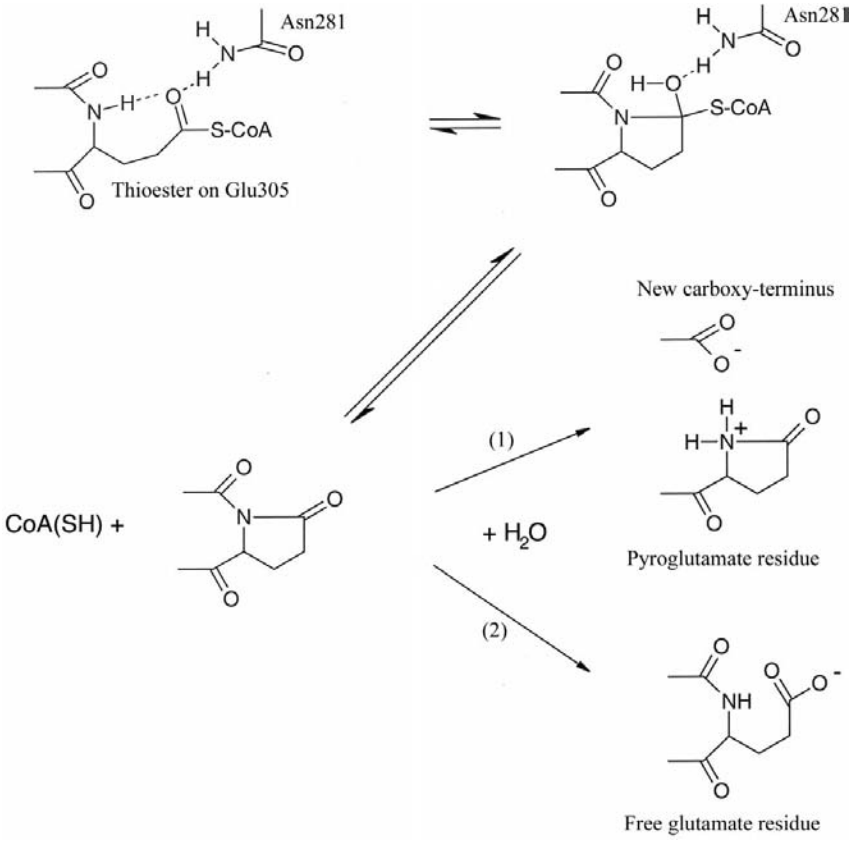

Figure 1
Mechanism for the autolytic fragmentation.

chain and leaving the glutamyl residue as a pyroglutamate residue at the newly formed amino-terminus.

The active-site glutamate residue adopts a different conformation in SCOT to that in GCT (Jacob *et al.*, 1997). The side chains that would facilitate the autolytic fragmentation in SCOT are not present in GCT. There is no asparagine residue equivalent to Asn281 in GCT: instead, Thr28β occupies this position. The hydroxyl group of Thr28β could only form a long and, therefore, weak hydrogen bond with the active-site glutamate side chain, even if the two were ideally oriented, which they are not. In the structure of GCT, Thr28β C$^{\gamma 2}$ is directed towards the active-site glutamate residue and the region is quite hydrophobic, with Ile52β in place of Gln303 of SCOT and Phe87β in place of Ser346 of SCOT. It may be that SCOT has evolved so that it can be fragmented and degraded in the absence of saturating concentrations of succinate or acetoacetate (Howard *et al.*, 1986). This may be one mode of regulating CoA transferase that is useful for its role in ketone-body metabolism.

The different conformations of the active-site glutamate residue that are seen in the structures of GCT and SCOT may be conformations that are adopted along the pathway of the catalytic mechanism. Catalytic roles for specific amino-acid residues at the active site of GCT were postulated by Jacob and coworkers based on that structure (Jacob *et al.*, 1997). In the conformation found in GCT, the glutamate side chain is within 3.5 Å of the side chain of Gln103α and of the main-chain N atom of Gly137β, leading Jacob and coworkers to suggest that the reaction with CoA is facilitated by hydrogen bonds to both of these N atoms. These same N atoms were also thought to form an oxyanion hole to stabilize the negative charge of the O atom of Glu305β in the tetrahedral intermediate. The N atom of Gly137β as well as the amide N atom of Ala138β were presented as possible candidates for stabilizing the oxyanion that is generated on the carboxylate group of the substrate. The glutamine residue is conserved in α-ACT, where it is Gln102α (Korolev *et al.*, 2002). SCOT has an equivalent glutamine residue, Gln99, as well as Gly386 and Ala387. If the free thiol of CoA reacts with SCOT in the same way that it reacts with GCT and if the hypotheses of Jacob and coworkers are correct, Glu305 must rotate about χ_2, displacing two water molecules that are located in the active site (Fig. 2). After reacting with CoA, the activated glutamyl residue could then rotate back to the position seen in our present structure. This movement of the glutamate side chain would require a slight shift of at least the pantothenate portion of CoA, since the positions of the O atoms that would have to be replaced by the S atom of CoA are approximately 1.3 Å apart in the two conformations.

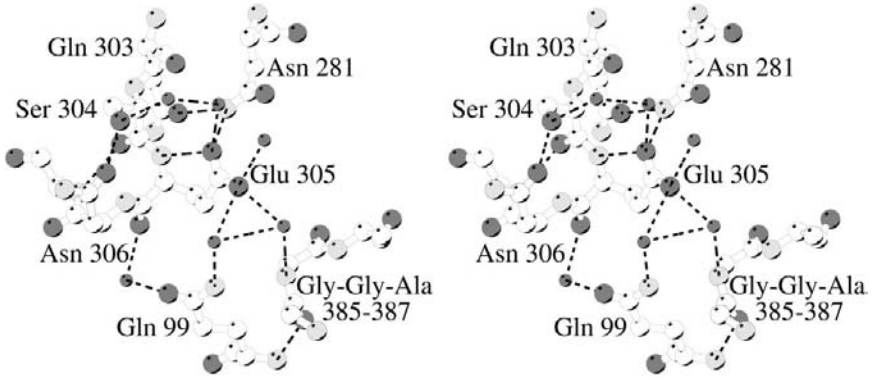

Figure 2
Active-site glutamate residue. In this stereoview, the conformations of the active-site glutamate residue and of surrounding residues and water molecules are shown using ball-and-stick models. The balls are shaded according the atom type, using darker shades for the heavier atoms, and the water molecules are drawn as small balls. The dashed lines represent hydrogen-bonding interactions. This figure as well as Figs. 3 and 5 were drawn using the program *MOLSCRIPT* (Kraulis, 1991).

Figure 3
Superposition of SCOT and α-ACT. The C$^{\alpha}$ trace is shown for α-ACT as dashed lines and for the first 242 residues of SCOT as a solid line. The label N is near the amino-termini of the two and the last C$^{\alpha}$ atom of SCOT that superposes well with α-ACT is numbered 231. The two monomers were superposed using the program *O* (Jones *et al.*, 1991) with a 2.9 Å cutoff.

3.3. Succinate- or acetoacetate-binding site

The comparison between the initial SCOT structure and the structure of GCT pointed out three charged residues in SCOT that might play a role in the binding of succinate or acetoacetate: Lys329, Glu241 and Arg242 (Bateman *et al.*, 2002). This interpretation was based on the different conformations of loops near the active site of the two CoA transferases.

The structure of the α-subunit of ACT (Korolev *et al.*, 2002) can be added to the comparison. ACT catalyzes the reaction acetyl-CoA + acetoacetate $\leftrightarrow$ acetoacetyl-CoA + acetate and is known to act on

butaryl-CoA but not succinyl-CoA (Sramek & Frerman, 1975). The substrates of ACT are more similar to those of SCOT than are the substrates of GCT. Unsurprisingly, the sequence identity between SCOT and ACT is higher than that between either of these CoA transferases and GCT. The superposition of SCOT and α-ACT is shown in Fig. 3 and the sequence alignment based on the structural superposition is given in Fig. 4. When only residues that superpose are considered, the sequence identity is 39%.

Close-up views of SCOT and of ACT in the region proposed to bind the carboxylate substrates are presented in Fig. 5. As an aid for comparing the enzymes, the β-subunit of ACT (β-ACT) was modelled based on the structure of SCOT (Peitsch, 1995, 1996; Guex & Peitsch, 1997). Fig. 5(*b*) is a hybrid of the structure of the α-subunit determined using crystallographic data and the structure of the β-subunit modelled from the crystal structure of SCOT. None of the three charged residues proposed to play a role in the binding of succinate or acetoacetate in SCOT is conserved in ACT. Glu241 and Arg242 are part of the linker region of SCOT that the bacterial enzymes do not possess. In the space occupied by the side chain of Lys329 of SCOT, ACT has a nonpolar residue, Met27α. This would be a quite logical difference if the positively charged Lys329 were to interact with the carboxylate group of succinate that is distal from CoA and the nonpolar Met27α were to interact with the nonpolar tail of the fatty-acid anion. There is a second lysine residue in this region of SCOT, Lys382, which aligns with another nonpolar residue, Pro120β of ACT. The same argument could be made for this pair of residues as for Lys329 and Met27α. One identical residue in the two structures is an asparagine residue: 51 in SCOT and 52α in ACT. In ACT, the side chain of Asn52α accepts a hydrogen bond from the conserved Gln102α, which suggests that a similar interaction is possible in SCOT. Korolev and coworkers pointed out that the tyrosine residue, Tyr74 in GCT, is not conserved in α-ACT, where a histidine residue is found instead (Korolev *et al.*, 2002). This would indicate that the tyrosine residue, which is conserved in SCOT, is not an essential residue for the catalytic mechanism of CoA transferases, but might play a role in the binding of substrate. An interesting difference between SCOT and α-ACT is that the peptide group between Gly78 and Glu79 is flipped relative to that between Gly79α and Thr80α. This could be a real difference between the two structures or it could indicate that a conformational change can occur and that the two structures have been crystallized in these two different conformations. Further work is necessary to determine the roles of the similar residues identified by this comparison of SCOT with ACT and to delineate the succinate- or acetoacetate-binding site of SCOT.

```
2      KFYTD 6
       *  *
4α     KLMTL 8α

12     KDIPNGATVLVGGFGLCGIPENLIGALLKTGVKELTAVSNNAGVDNFGLG
       * *  ****   * *  *  ***  **  **   *       * *
13α    GFFRDGMTIMVGGFMGIGTPSRLVEALLESGVRDLTLIANDTAFVDTGIG

62     LLLQSKQIKRMISSYVGENAEFERQYLAGELEVELTPQGTLAERIRAGGA
       *         * *  * * *  *    **  * * ***** * ** ***
63α    PLIVNGRVRKVIASHIGTNPETGRRMISGEMDVVLVPQGTLIEQIRCGGA

112    GVPAFYTSTGYGTLVQE 128
       *   * * ** ** * *
113α   GLGGFLTPTGVGTVVEE 129α

147    PREVREFNGQHFILEEAIRGDFALVKAWKADQAGNVTFRKSARNFNLPMC
       *    **   * * **  *   *  ** *   ******
130α   GKQTLTLDGKTWLLERPLRADLALIRAHRCDTLGNLTYQLSARNFNPLIA

197    KAAETTVVEVEEIVDIGSFAPEDIHIPKIYVHRLV 231
       **  * **  * *  *   *  *  *
180α   LAADITLVEPDELVETGELQPDHIVTPGAVIDHII 214α
```

Figure 4
Alignment of SCOT and α-ACT based on the structural superposition shown in Fig. 3. Only the residues that superpose are listed. The residue numbers are presented at the beginning and the end of each stretch of superposed polypeptide chain.

3.4. Ion-binding sites in SCOT

Five ions have been modelled in the high-resolution structure of SCOT. Four are potassium ions and the other is a phosphate ion. All are proposed to come from the phosphate buffer used in the crystallization.

The four potassium ions are actually two pairs of ions, one pair bound to each of the monomers. The best defined pair is bound to chain *A*. The electron density for the pair bound to chain *B*, as well as for the phosphate ion and the surrounding residues, is shown in Fig. 6 since the phosphate ion binds near the pair that is bound to chain *B*. The two ions bound to chain *A* were identified as potassium ions by the low temperature factors that were obtained when they were refined as water molecules. The distances between the ions and the protein atoms to which they are coordinated, as well as their coordination numbers, support their identification as potassium ions (Harding, 2002). The first potassium ion is coordinated by the carbonyl O atoms of Lys424 and Gln425 and by four or five water molecules. The second ion, located only 6.5 Å from the first, is coordinated by the carbonyl O atoms of Ser393, Ala394, Thr396 and Cys426, by the side-chain atom OD1 of Asn428 and by two water molecules. The electron density is elongated and the distances are long between the potassium ion and both Cys426 and Ala394, which are at apical coordination sites, suggesting that the ion has refined to an intermediate position.

The phosphate ion is located in the same crevice as the pair of potassium ions that are bound to chain *B*. The phosphate ion is within 5 Å of one of the potassium ions and it is coordinated to one of the water molecules that this potassium ion coordinates. One of the phosphate O atoms accepts hydrogen bonds from both ND1 and the main-chain N atom of His157. A water molecule is modelled in the electron density

at a similar position in chain *A*. Although the potassium ions are only bound to residues in the carboxy-terminal portion of SCOT, the phosphate ion is bound to a residue of the amino-terminal portion; together, they form a bridge between the two portions of SCOT.

None of the ions is bound near the active site, so there is no indication that they would affect catalysis. However, the use of the phosphate buffer does result in the nucleation and growth of this orthorhombic crystal form and these ion-binding sites may be important for the crystallization. The phosphate ion is located near a dimer–dimer interface.

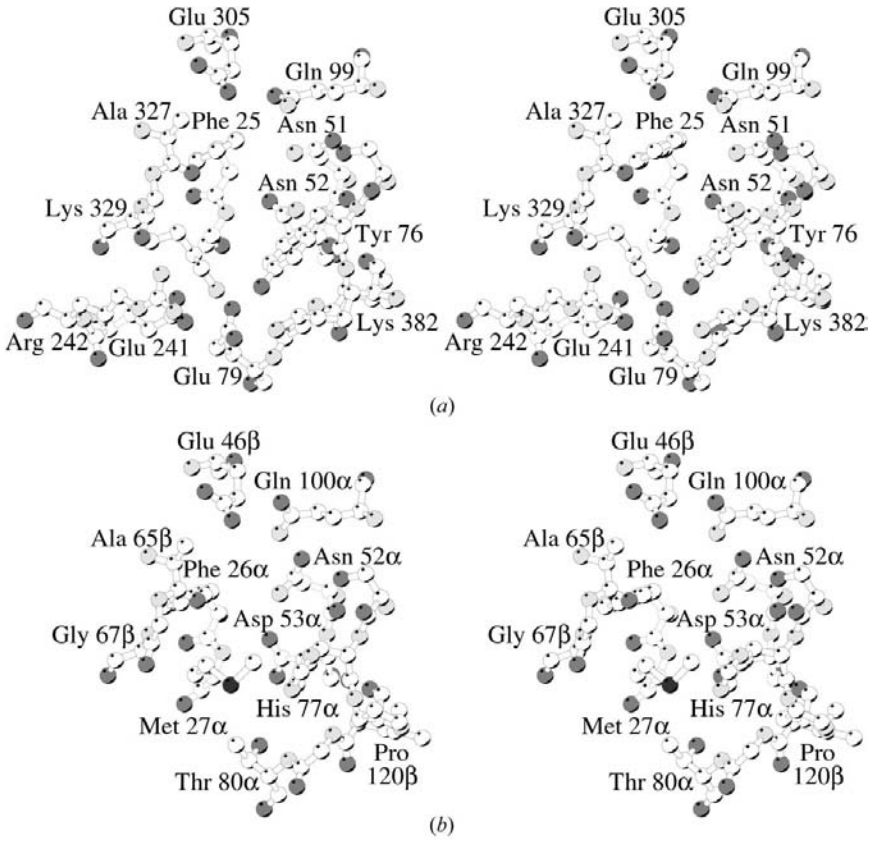

Figure 5
Proposed substrate-binding site. (*a*) SCOT, (*b*) ACT. In these stereoviews, the residues that might interact with the carboxylate substrates are shown using ball-and-stick models. The balls are shaded according to the atom type, using darker shades for the heavier atoms. Since the structure of β-ACT has not been determined crystallographically, this subunit was modelled based on the structure of SCOT (Peitsch, 1995, 1996; Guex & Peitsch, 1997).

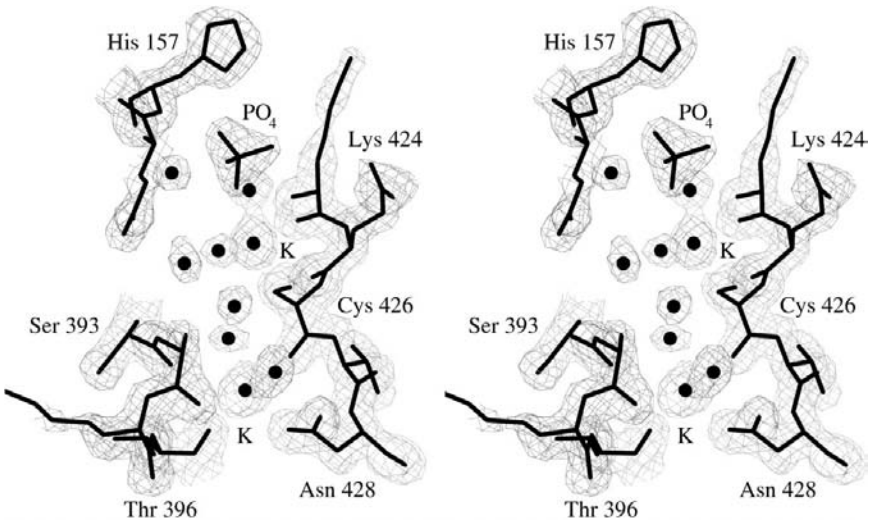

Figure 6
Electron density at the ion-binding sites. The electron density for the three ions bound to chain *B* of SCOT, two potassium ions (labelled K), the phosphate ion (labelled PO_4) and the surrounding residues and water molecules is shown in this stereoview. The electron density is that of the $2F_o - F_c$, α_c map contoured at 1σ. This figure was drawn using the programs *BOBSCRIPT* (Esnouf, 1997) and *MOLSCRIPT* (Kraulis, 1991).

3.5. Quaternary structure

In the orthorhombic crystal form of SCOT, two dimers pack together at a crystallographic twofold axis to form a tetramer. This tetramer is shown in Fig. 7(*a*). A question that needs to be answered is whether this is the physiologically relevant tetramer. It had been shown that CoA transferase partially purified from pig heart tissue exists in both a dimeric and a tetrameric form (Rochet *et al.*, 2000). Our initial crystal structure showed the structure of the dimer (Bateman *et al.*, 2002). Since both the dimeric form and the tetrameric form have the same specific activity in solution (Rochet *et al.*, 2000), the structure of the dimer is sufficient for analysis of the catalytic mechanism of the enzyme in solution. However, since the quaternary structure is likely to be relevant for interactions with other proteins in the mitochodria where CoA transferase functions, the structure of the tetramer is also of interest.

It was expected that the dimer–dimer interface in the SCOT tetramer would involve residues of the linker region (Rochet *et al.*, 2000). The rationale behind this idea, presented in Rochet *et al.* (2000), is as follows. The tetramer dissociated in solutions containing salt, so it was concluded that electrostatic forces are important at the dimer–dimer interface. The linker region includes many polar residues, including a large number of charged residues, so it was targeted for study. A mutant in which the amino-terminal portion and the carboxy-terminal portion of SCOT were produced as separate polypeptide chains is produced in *E. coli* only as the dimer. However, ΔSCOT, the deletion mutant lacking six residues of the linker, is produced as both the dimer and the tetramer, but with a lower fraction in

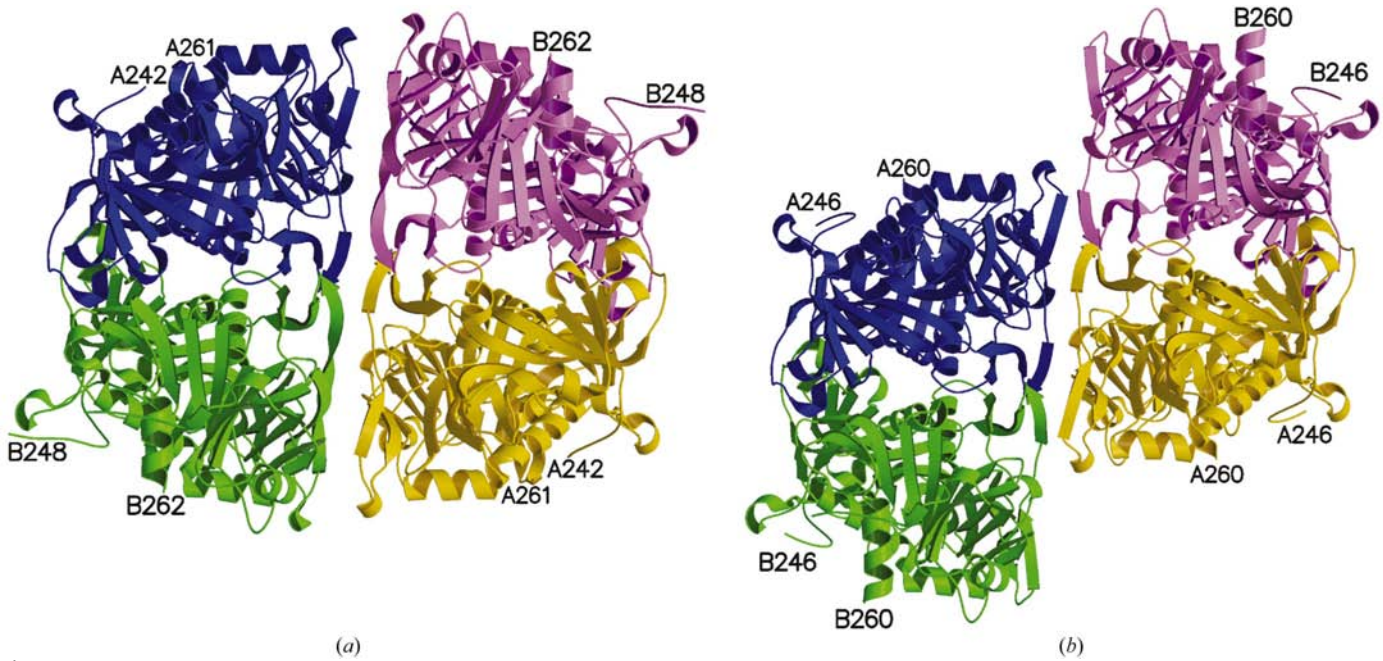

Figure 7
Quaternary structure. (*a*) Wild-type CoA transferase, SCOT. (*b*) The deletion mutant, ΔSCOT, in space group $P2_12_12$. The tetramers formed by the packing two dimers at a crystallographic twofold axis. This figure was drawn using the programs *MOLSCRIPT* and *RASTER3D* (Kraulis, 1991; Merritt & Bacon, 1997).

the tetrameric form than exists for SCOT. Surprisingly, the tetramer seen in the crystals (Fig. 7*a*) does not involve residues of the linker region. Also, although ΔSCOT crystallized in the monoclinic *C*2 crystal form does show the same packing, ΔSCOT crystallized in the orthorhombic crystal form uses the same face of the dimer at the dimer–dimer interface, but different residues (Fig. 7*b*).

The characteristics of the residues at the dimer–dimer interface in the tetramer are in favour of the view that this is the physiologically relevant tetramer. The dimer–dimer interface in the tetramer is expected to have charged groups since the tetramer dissociates in the presence of the salt potassium chloride (Rochet *et al.*, 2000). At the centre of each side of the interface is the noncrystallographic twofold axis that relates one monomer to the other in the dimer. This means that every interaction appears twice. Glu149 and Arg151 from one monomer form ionic bonds with Arg151 and Glu149, respectively, from the other monomer. Within the rectangle that they delineate are several water molecules, which also form hydrogen bonds with the hydroxyl groups contributed by the two Tyr117 residues from the layer below the surface. The two dimers are approximately 3.5 Å apart, with more water molecules sandwiched between them. It is easy to imagine how this packing would be disrupted by salt, since the salt would have access *via* the layer of water molecules and would then shield the electrostatic interactions between the two dimers. Each phosphate ion binds only to residues on one side of the interface, but the two phosphate ions would affect electrostatic interactions at the interface.

The hypothesis that this is the physiologically relevant tetramer could be tested *via* mutagenesis of residues at the interface or *via* small-angle X-ray scattering by the tetramer.

We would like to thank Edward Brownie for his technical assistance in protein production and purification, Dr Robert Sweet for guidance at beamline X12C and the BioCARS team for guidance at beamline 14-BM-C. The Canadian Institutes of Health Research funded this research through grant MOP-42446. MEF is a Biomedical Scholar supported by the Alberta Heritage Foundation for Medical Research (AHFMR). Computational resources were purchased with an Establishment Grant from AHFMR and an Equipment Grant from the Natural Sciences and Engineering Research Council of Canada. Data for this study were measured at beamline X12C of the National Synchrotron Light Source and at the BioCARS beamline 14-BM-C of the Advanced Photon Source. Financial support for beamline X12C comes principally from the National Center for Research Resources of the National Institute of Health and from the Offices of Biological and Environmental Research and of Basic Energy Sciences of the US Department of Energy. Use of the Advanced Photon Source was supported by the US Department of Energy, Basic Energy Sciences, Office of Science under Contract No. W-31-109-Eng-38. Use of the BioCARS Sector 14 was supported by the National Institutes of Health, National Center for Research Resources under grant No. RR07707. The Alberta Synchrotron Institute supported WTW's travel to the Advanced Photon Source.

References

Bateman, K. S., Brownie, E. R., Wolodko, W. T. & Fraser, M. E. (2002). *Biochemistry*, **41**, 14455–14462.
Benson, R. W. & Boyer, P. D. (1969). *J. Biol. Chem.* **244**, 2366–2371.

Berman, H. M., Westbrook, J., Feng, Z., Gilliland, G., Bhat, T. N., Weissig, H., Shindyalov, I. N. & Bourne, P. E. (2000). *Nucleic Acids Res.* **28**, 235–242.
Brünger, A. T., Adams, P. D., Clore, G. M., DeLano, W. L., Gros, P., Grosse-Kunstleve, R. W., Jiang, J.-S., Kuszewski, J., Jilges, N., Pannu, N. S., Read, R. J., Rice, L. M., Simonson, T. & Warren, G. L. (1998). *Acta Cryst.* D**54**, 905–921.
Buckel, W., Dorn, U. & Semmler, R. (1981). *Eur. J. Biochem.* **118**, 315–321.
Collaborative Computational Project, Number 4 (1994). *Acta Cryst.* D**50**, 760–763.
Esnouf, R. M. (1997). *J. Mol. Graph.* **15**, 132–134.
Guex, N. & Peitsch, M. C. (1997). *Electrophoresis*, **18**, 2714–2723.
Harding, M. M. (2002). *Acta Cryst.* D**58**, 872–874.
Hersh, L. B. & Jencks, W. P. (1967). *J. Biol. Chem.* **242**, 3468–3480.
Hooft, R. W. W., Vriend, G., Sander, C. & Abola, E. E. (1996). *Nature (London)*, **381**, 272.
Howard, J. B., Zieske, L., Clarkson, J. & Rathe, L. (1986). *J. Biol. Chem.* **261**, 60–65.
Jacob, U., Mack, M., Clausen, T., Huber, R., Buckel, W. & Messerschmidt, A. (1997). *Structure*, **5**, 415–426.
Jones, T. A. (1985). *Methods Enzymol.* **115**, 157–171.
Jones, T. A., Zou, J. Y., Cowan, S. W. & Kjeldgaard, M. (1991). *Acta Cryst.* A**47**, 110–119.
Kassovska-Bratinova, S., Fukao, T., Song, X.-Q., Duncan, A. M. V., Chen, H. S., Robert, M.-F., Pérez-Cerdá, C., Ugarte, M., Chartrand, C., Vobecky, S., Kondo, N. & Mitchell, G. A. (1996). *Am. J. Hum. Genet.* **59**, 519–528.
Korolev, S., Koroleva, O., Petterson, K., Gu, M., Collart, F., Dementieva, I. & Joachimiak, A. (2002). *Acta Cryst.* D**58**, 2116–2121.
Kraulis, P. J. (1991). *J. Appl. Cryst.* **24**, 946–950.
Laskowski, R. A., MacArthur, M. W., Moss, D. S. & Thornton, J. M. (1993). *J. Appl. Cryst.* **26**, 283–291.
Lin, T. W. & Bridger, W. A. (1992). *J. Biol. Chem.* **267**, 975–978.
Lloyd, A. J. & Shoolingin-Jordan, P. M. (2001). *Biochemistry*, **40**, 2455–2467.
Mack, M. & Buckel, W. (1995). *FEBS Lett.* **357**, 145–148.
Merritt, E. A. & Bacon, D. J. (1997). *Methods Enzymol.* **277**, 505–524.
Navaza, J. (1994). *Acta Cryst.* A**50**, 157–163.
Niezen-Koning, K. E., Wanders, R. J. A., Ruiter, J. P. N., Ijlst, L., Visser, G., Reitsma-Bierens, W. C. C., Heymans, H. S. A., Reijngoud, D. J. & Smit, G. P. A. (1997). *Eur. J. Pediatr.* **156**, 870–873.
Otwinowski, Z. & Minor, W. (1997). *Methods Enzymol.* **276**, 307–326.
Peitsch, M. C. (1995). *Biotechnology*, **13**, 658–660.
Peitsch, M. C. (1996). *Biochem. Soc. Trans.* **24**, 274–279.
Pretorius, C. J., Loy Son, G. G., Bonnici, F. & Harley, E. H. (1996). *J. Inher. Metab. Dis.* **19**, 296–300.
Read, R. J., Fujinaga, M., Sielecki, A. R. & James, M. N. G. (1983). *Biochemistry*, **22**, 4420–4433.
Rochet, J. C. & Bridger, W. A. (1994). *Protein Sci.* **3**, 975–981.
Rochet, J. C., Brownie, E. R., Oikawa, K., Hicks, L. D., Fraser, M. E., James, M. N. G., Kay, C. M., Bridger, W. A. & Wolodko, W. T. (2000). *Biochemistry*, **39**, 11291–11302.
Selmer, T. & Buckel, W. (1999). *J. Biol. Chem.* **274**, 20772–20778.
Snyderman, S. E., Sansaricq, C. & Middleton, B. (1998). *Pediatrics*, **101**, 709–711.
Solomon, F. & Jencks, W. P. (1969). *J. Biol. Chem.* **244**, 1079–1081.
Sramek, S. J. & Frerman, F. E. (1975). *Arch. Biochem. Biophys.* **171**, 14–26.
Stern, J. R., Coon, M. J., del Campillo, A. & Schneider, M. C. (1956). *J. Biol. Chem.* **221**, 15–31.
Tong, L. & Rossmann, M. G. (1990). *Acta Cryst.* A**46**, 783–792.
White, H., Solomon, F. & Jencks, W. P. (1976). *J. Biol. Chem.* **251**, 1700–1707.
Williams, W. A. (1990). PhD thesis, University of Minnesota, USA.